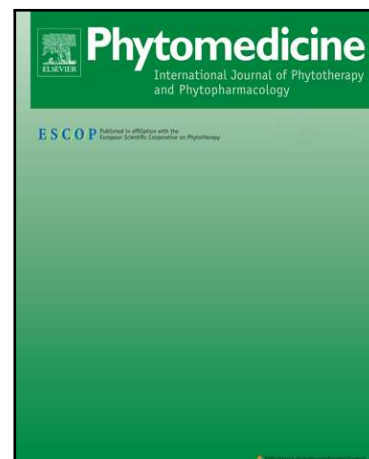


## Accepted Manuscript



Cholinesterase-inhibitory effect and in silico analysis of alkaloids from bulbs of Hieronymiella species

Javier E. Ortiz , Adriana Garro , Natalia B. Pigni ,  
María Belén Agüero , German Roitman , Alberto Slanis ,  
Ricardo D. Enriz , Gabriela E. Feresin , Jaume Bastida ,  
Alejandro Tapia

PII: S0944-7113(17)30194-0  
DOI: [10.1016/j.phymed.2017.12.020](https://doi.org/10.1016/j.phymed.2017.12.020)  
Reference: PHYMED 52322

To appear in: *Phytomedicine*

Received date: 1 March 2017  
Revised date: 26 October 2017  
Accepted date: 19 December 2017

Please cite this article as: Javier E. Ortiz , Adriana Garro , Natalia B. Pigni , María Belén Agüero , German Roitman , Alberto Slanis , Ricardo D. Enriz , Gabriela E. Feresin , Jaume Bastida , Alejandro Tapia , Cholinesterase-inhibitory effect and in silico analysis of alkaloids from bulbs of Hieronymiella species, *Phytomedicine* (2017), doi: [10.1016/j.phymed.2017.12.020](https://doi.org/10.1016/j.phymed.2017.12.020)

This is a PDF file of an unedited manuscript that has been accepted for publication. As a service to our customers we are providing this early version of the manuscript. The manuscript will undergo copyediting, typesetting, and review of the resulting proof before it is published in its final form. Please note that during the production process errors may be discovered which could affect the content, and all legal disclaimers that apply to the journal pertain.

# Cholinesterase-inhibitory effect and *in silico* analysis of alkaloids from bulbs of *Hieronymiella* species

Javier E. Ortiz<sup>a</sup>, Adriana Garro<sup>b</sup>, Natalia B. Pigni<sup>c,f</sup>, María Belén Agüero<sup>a</sup>, German Roitman<sup>d</sup>, Alberto Slanis<sup>e</sup>, Ricardo D. Enriz<sup>b</sup>, Gabriela E. Feresin<sup>a,1</sup>, Jaume Bastida<sup>f</sup>, Alejandro Tapia<sup>a,1,\*</sup>

<sup>a</sup>*Instituto de Biotecnología-Instituto de Ciencias Básicas, CONICET, Facultad de Ingeniería, Universidad Nacional de San Juan, Av. Libertador General San Martín 1109 (O), CP 5400, San Juan, Argentina*

<sup>b</sup>*Facultad de Química, Bioquímica y Farmacia, Universidad Nacional de San Luis, Chacabuco 915, 5700 San Luis, Argentina*

<sup>c</sup>*ICYTAC-CONICET, Departamento de Química Orgánica, Facultad de Ciencias Químicas, Universidad Nacional de Córdoba, 5000, Córdoba, Argentina*

<sup>d</sup>*Cátedra de Jardinería, Facultad de Agronomía, Universidad de Buenos Aires, Av. San Martín 4453, 1417 Buenos Aires, Argentina*

<sup>e</sup>*Facultad de Ciencias Naturales e Instituto Miguel Lillo, Universidad Nacional de Tucumán, Fundación Miguel Lillo 251, Tucumán, Argentina*

<sup>f</sup>*Departament de Productes Naturals, Biologia Vegetal i Edafologia, Facultat de Farmàcia, Universitat de Barcelona, Avda. Joan XXIII s/n, 08028 Barcelona, Spain*

<sup>1</sup>The work was co-directed by both authors

\*Corresponding author

Instituto de Biotecnología, Facultad de Ingeniería, Universidad Nacional de San Juan, Av. Libertador General San Martín 1109 (O), CP 5400, San Juan, Argentina Tel: +54 264 4211700 int. 410; fax: +54 264 4213672.

E-mail address: atapia@unsj.edu.ar (A. Tapia)

**ABSTRACT**

**Background:** In Argentina, the Amaryllidaceae family (59 species) comprises a wide variety of genera, only a few species have been investigated as a potential source of cholinesterases inhibitors to treat Alzheimer disease (AD).

**Purpose:** To study the acetylcholinesterase (AChE) and butyrylcholinesterase (BChE) inhibitory activities of the basic dichloromethane extracts (E) from *Hieronimiella aurea*, *H. caletensis*, *H. clidanthoides*, *H. marginata*, and *H. speciosa* species, as well as the isolated compounds from these plant extracts.

**Study design and methods:** AChE and BChE inhibitory activities were evaluated with the Ellman's spectrophotometric method. The alkaloids composition from the E was obtained by gas chromatography-mass spectrometry (GC-MS). The E were successively chromatographed on a silica gel column and permeated on Sephadex LH-20 column to afford the main alkaloids identified by means of spectroscopic data. Additionally, an *in silico* study was carried out.

**Results:** Nine known alkaloids were isolated from the E of five *Hieronimiella* species. Galanthamine was identified in all the species by GC-MS standing out *H. caletensis* with a relative abundance of 9.79% of the total ion current. Strong AChE ( $IC_{50} = 1.84 - 15.40 \mu\text{g/ml}$ ) and moderate BChE ( $IC_{50} = 23.74 - 136.40 \mu\text{g/ml}$ ) inhibitory activities were displayed by the extracts. Among the isolated alkaloids, only sanguinine and chlidanthine (galanthamine-type alkaloids) demonstrated inhibitory activity toward both enzymes. The QTAIM study suggests that sanguinine has the strongest affinity towards AChE, attributed to an additional interaction with Ser200 as well as stronger molecular interactions Glu199 and His440. These results allowed us to differentiate the molecular behavior in the active site among alkaloids possessing different *in vitro* inhibitory activities.

**Conclusion:** *Hieronimiella* species growing in Argentina represent a rich and widespread source of galanthamine and others AChE and BChE inhibitors alkaloids. Additionally, the new trend towards the use of natural extracts as pharmaceuticals rather than pure drugs opens a pathway for the development of a phytomedicine derived from extracts of *Hieronimiella spp.*

**Keywords:** Amaryllidaceae, *Hieronimiella*, Cholinesterases, *In silico*, Alkaloids, Argentina

**Abbreviations:** AChE, acetylcholinesterase enzyme; BChE, butyrylcholinesterase enzyme; E, extracts

## Introduction

The genus *Hieronymiella*, which belongs to the Amaryllidaceae family, is native to Argentina and comprises five species *H. aurea*, *H. caletensis*, *H. clidanthoides*, *H. marginata*, and *H. speciosa* (Arroyo-Leuenberger and Dutilh, 2008). To the best of our knowledge, no previous reports about phytochemical studies and bioactive properties have been performed in these species.

The Amaryllidaceae family is an important source of alkaloids with a wide range of biological activities including acetylcholinesterase (AChE) and butyrylcholinesterase (BChE) inhibitory effects (Bastida et al., 2011; Kulhánková et al., 2013; Cavallaro et al., 2014; Ortiz et al., 2016).

Galanthamine (Gal) is a long-acting, selective, reversible, and competitive AChE inhibitor exclusively produced by Amaryllidaceae family and currently used for the treatment of Alzheimer's disease (AD) (Bastida et al., 2011). Likewise, Gal has shown inhibitory activity against BChE, a legitimate therapeutic target for ameliorating the cholinergic deficit considered to be responsible, for the declines in cognitive, behavioral, and global functioning characteristics of AD (Greig et al., 2002; Anand and Singh, 2013; Zhao et al. 2013).

In an effort to search for new sources of cholinesterases inhibitors, the phytochemical study of *Hieronymiella* species was conducted. Thus, the enriched alkaloid extracts from the bulbs as well as the isolated alkaloids were evaluated for *in vitro* cholinesterase-inhibitory activities. For further insight into the experimental results, a molecular modeling study was carried out.

## Materials and methods

### *General experimental procedures*

NMR spectra were performed on Mercury 400 MHz (Palo Alto, CA, USA) and a Varian 500 MHz (Palo Alto, CA, USA) instrument using CDCl<sub>3</sub> and CD<sub>3</sub>OD as solvents. All 2D NMR experiments were performed using standard pulse sequences. GC-MS analysis of alkaloid extracts were performed on a Agilent 6890N GC 5975 instrument (Agilent Technologies, Santa Clara, CA, USA) operating in EI mode at 70 eV. A DB-5 MS column (30 m x 0.25 mm x 0.25 μm) was used. The temperature program was: 100-180 °C at 15 °C min<sup>-1</sup>, 1 min hold at 180 °C, 180-300 °C at 5 °C min<sup>-1</sup>, and 1 min hold at 300 °C. The injector temperature was 280 °C. The flow rate of carrier gas (He) was 0.8 ml min<sup>-1</sup>. The split ratio was 1:20. The results obtained were analyzed using AMDIS 2.64 software. Compounds were identified through the comparison of their mass spectral patterns and retention index (RI) with those of previously isolated alkaloids. RIs were calculated through calibration with a standard *n*-hydrocarbon mixture (C<sub>9</sub>–C<sub>36</sub>). Results are expressed as a percentage of

total ion current (TIC) in each chromatogram, which was used for comparison of relative abundance between components of the extract. HRESIMS data were obtained via LC/MSD-TOF (Agilent 2006) (Agilent Technologies) by direct injection of the compounds dissolved in MeOH. All solvents used were of analytical grade. Chloroform was purchased from Fisher (USA); methanol (MeOH) from J.T. Baker (USA). Ultra pure water ( $< 5 \mu\text{g/L}$ ) was obtained from a purification system Arium 61316-RO plus Arium 611 UV (Sartorius, Germany). Sephadex LH-20 column (column length 20 cm, diameter 2.5 cm) was equilibrated and then permeated with PE:MeOH:CHCl<sub>3</sub> (2:1:1). Column chromatography (CC) was performed using silica gel 60A (6–35  $\mu\text{m}$ ). For analytical and preparative TLC, Merck Sílicagel 60 F<sub>254</sub> was carried out. The bands were detected by UV light, iodine vapors resublimed, and staining with Dragendorff's reagent.

#### *Plant material*

Bulbs from eight samples belonging to five species: *Hieronymiella aurea* Ravenna, *H. caletensis* Ravenna, *H. clidanthoides* Pax (two samples), *H. marginata* (Pax) Hunz (three samples), and *H. speciosa* (R.E. Fr.) Hunz were collected in different sites, in the provinces of Tucumán, Salta, Jujuy, and La Rioja (Argentina) during the flowering period between December 2012 and March 2013. The species were authenticated by MCS German Roitman (Facultad de Agronomía, Universidad de Buenos Aires, Argentina) and then deposited in the herbarium of Universidad de Buenos Aires under an specific herbarium code as follows: IBT-Arg 7 (*H. aurea*, from Los Cardones, Salta); IBT-Arg 8 (*H. caletensis*, from Tilcara, Jujuy); IBT-Arg 9 (*H. clidanthoides*, from Los Quilmes, Tucumán); IBT-Arg 10 (*H. clidanthoides*, from Chepes, La Rioja); IBT-Arg 11 (*H. marginata*, from Tafí del Valle, Tucumán); IBT-Arg 12 (*H. marginata*, from El Volcán, Jujuy); IBT-Arg 13 (*H. marginata*, from Tumbaya, Jujuy); and IBT-Arg 14 (*H. speciosa*, from San Antonio de los Cobres, Salta).

#### *Extraction and isolation*

Dry powdered bulb material (100-300 g, depending on the species) was macerated in H<sub>2</sub>SO<sub>4</sub> 2% for 4 h in ultrasonic bath (3 × 1000 ml). Subsequently, samples were centrifuged at 5000 rpm (10 min), and the supernatant was transferred to another flask where it was defatted with diethylether (3 × 500 ml). The aqueous solution was led to pH 11-12 with 10% NaOH and the alkaloids were extracted with dichloromethane (3 × 500 ml). The organic phase was dried with anhydrous sodium sulfate and then evaporated to obtain the basic dichloromethane extracts named as HE1 (*H. aurea*), HE2 (*H. caletensis*), HE3 (*H. clidanthoides*, Los Quilmes), HE4 (*H. clidanthoides*, Chepes), HE5 (*H. marginata*, Tafí del Valle), HE6 (*H. marginata*, El Volcán), HE7 (*H. marginata*, Tumbaya), and HE8 (*H. speciosa*).

*H. aurea* extract (HE1)

The HE1 (380 mg, yield extract w/w: 0.32%) was dissolved in MeOH (3 ml) and permeated with MeOH in a Sephadex LH-20 column (51 cm length, 5 cm i.d.) to give twenty fractions. After TLC ( $\text{Cl}_3\text{CH}/\text{MeOH}/\text{NH}_3$ , 90:9:1) comparison, fractions with similar retention factor were combined to give five subfractions (I–V): **I** (1): 26.8 mg, **II** (2-5): 170 mg, **III** (6-9): 60.3 mg, **IV** (10-12): 43.9 mg, and **V** (13-20): 72 mg. Fraction **II** was consecutively chromatographed on a silica gel column (CC) using gradient elution from *n*-hexane/EtOAc (2:8–0:10) to EtOAc/MeOH (9:1) to afford 15 mg of haemanthamine (**11**) and 8 mg of crinamine (**12**), while fraction **IV** gave 5 mg of lycorine (**18**) by precipitation.

*H. caletensis* extract (HE2)

Column on Sephadex LH-20 (permeated with MeOH, 51 cm length, 5 cm i.d.) of HE2 (310 mg, yield extract w/w: 0.28%) dissolved in MeOH (2.5 ml) gave twelve fractions. After TLC comparison fractions with similar TLC patterns were combined in four subfractions (I–IV): **I** (1-3): 66 mg, **II** (4-5): 73.4 mg, **III** (6-8): 82.5 mg, and **IV** (9-12): 83.9 mg. Consecutively, fraction **III** was permeated with MeOH through Sephadex LH-20 column (30 cm length, 2.5 cm i.d.) giving ten subfractions, whereas subfractions 4-6 were combined and subjected to preparative TLC ( $\text{Cl}_3\text{CH}/\text{MeOH}/\text{NH}_3$ , 90:9:1), to afford 5 mg of Gal (**2**). Fraction **IV** gave 20 mg of lycorine (**18**) by direct precipitation.

*H. clidanthoides* extract (HE3) (sample from Los Quilmes, Tucumán)

The HE3 (410 mg, yield extract w/w: 0.31%) was roughly separated by  $\text{SiO}_2$  flash CC (10 cm length, 5 cm i.d.) using an *n*-hexane/EtOAc/ $\text{CH}_2\text{Cl}_2$ /MeOH gradient to give five fractions: **I** (*n*-hexane/EtOAc, 1:4) 80 mg, **II** (EtOAc) 120 mg, **III** (EtOAc/ $\text{CH}_2\text{Cl}_2$ , 1:1) 78 mg, **IV** (EtOAc/MeOH, 9.5:0.5) 50 mg, and **V** (EtOAc/MeOH, 9:1) 60 mg. Fraction **II** was applied onto a Sephadex LH-20 column (length 40 cm, 4 cm i.d., MeOH) to give twelve fractions. After TLC comparison, fractions with similar retention factor were combined to give three subfractions (**IIa–IIc**). Fraction **IIb** (80 mg) was subjected to preparative TLC ( $\text{Cl}_3\text{CH}/\text{MeOH}/\text{NH}_3$ , 90:9:1) to afford hamayne (**15**) (10 mg) and 11-hydroxyvittatine (**16**) (4 mg).

*H. marginata* extract (HE5) (sample from Tafi del Valle, Tucumán)

The HE5 (520 mg, yield extract w/w: 0.32%) was dissolved and then permeated with MeOH through a Sephadex LH-20 column (51 cm length, 5 cm i.d.) affording fifteen fractions. After TLC comparison, fractions with similar patterns were combined to give four subfractions (I–IV): **I** (1-3):

95 mg, **II** (4-6): 150 mg, **III**: (7-8) 200 mg, and **IV** (9-10): 55 mg. Fraction **II** and fraction **III** were dissolved and then permeated with PE/MeOH/CH<sub>2</sub>Cl<sub>2</sub> (50:25:25) onto a Sephadex LH-20 column (length 35.5 cm, 2.5 cm i.d.). Fraction **II** yielded 15 mg of tazettine (**13**), while fraction **III** gave eight fractions. Fractions 5-7 were pooled and subjected to preparative TLC (silica gel with *n*-hexane/EtOAc/CHCl<sub>3</sub>/MeOH, 35:40:20:5, in NH<sub>3</sub> atmosphere) to afford 4 mg of sanguinine (**4**).

*H. marginata* extract (HE6) (sample from El Volcán, Jujuy)

The HE6 (360 mg, yield extract w/w: 0.14%) afforded 97 mg of lycorine by direct precipitation. Then, the extract was subjected to CC eluted with a EtOAc/MeOH gradient to afford 120 fractions, which were combined to give four groups of subfractions (**I-IV**): **I** (5-20, EtOAc/MeOH, 3:1) 30 mg, **II** (21-45, EtOAc/MeOH 1:1) 34 mg, **III** (46-102, EtOAc/MeOH 1:3) 125 mg, and **IV** (103-120, MeOH) 59 mg. Fraction **III** was permeated through a Sephadex LH-20 column (30 cm length, 2.5 cm i.d.) giving twelve fractions, whereas 5-8 were combined and then subjected to preparative TLC to afford 6 mg of chlidanthine (**3**). Fraction **IV** yielded 20 mg of lycorine (**18**) by direct precipitation.

Isolated alkaloids were identified by direct comparison of their spectroscopic properties (<sup>1</sup>H and <sup>13</sup>C NMR) with those of authentic samples obtained from other plant sources and the reported data (Likhitwitayawuid et al., 1993; Viladomat et al., 1994; Bastida et al. 1995, 2006, 2011). The chemical structures of the isolated alkaloids are shown in Fig. 1, while the chromatograms indicating the peaks corresponding to the isolated alkaloids are shown into supplementary material (Fig. 1S).

Insert Fig. 1

#### *Acetylcholinesterase and butyrylcholinesterase inhibitory bioassay*

Cholinesterase inhibitory activities were evaluated according to Ellman et al. (1961) with some modifications (Ortiz et al., 2016). The AChE and BChE activity assay was carried out using acetylthiocholine iodide and butyrylthiocholine iodide as substrates, respectively. Briefly, 50 µL of AChE or BChE in buffer phosphate (8 mM K<sub>2</sub>HPO<sub>4</sub>, 2.3 mM NaH<sub>2</sub>PO<sub>4</sub>, 0.15 M NaCl, pH 7.6) and 50 µL of the sample dissolved in the same buffer, were added to the wells of a microplate. The plates were incubated for 30 min at room temperature before the addition of 100 µL of the substrate solution (0.1 M Na<sub>2</sub>HPO<sub>4</sub>, 0.5 M DTNB, 0.6 mM ATCI in Millipore water, pH 7.5). The absorbance was read in a Thermo scientific multiskan FC microplate photometer at 405 nm after 5 min. Enzyme inhibitory activity was calculated as a percentage compared to an assay using buffer without any

inhibitor. The results obtained were analyzed with the software package Prism (Graph Pad Inc., San Diego, CA, USA). The values were expressed as half-maximal inhibitory concentration  $IC_{50}$  ( $\mu\text{g/ml}$  for extracts and  $\mu\text{M}$  for compounds), and were calculated as means  $\pm$  SD of 3 individual determinations. The enzymes AChE from the electric eel *Electrophorus electricus* and BChE from equine serum (Sigma-Aldrich) were used. Galanthamine (Sigma-Aldrich) was used as a positive control.

### *Molecular modeling*

#### *Automated docking setup.*

An X-ray structure available in the Protein Data Bank (<http://www.rcsb.org>) was used as follows: TcAChE (1DX6) (Greenblatt et al., 1999) and eqBChE (UniProtAC Q9N1N9). Molecular docking was conducted using AutoDock 4 (Trott and Olson, 2010). This program was adopted to perform molecular docking; the receptor structure was defined as rigid, and the grid dimensions were 50, 40, and 60 for the X, Y, and Z axes, respectively, in the catalytic site region with a resolution of 0.375 Å. Gasteiger charges were assigned for all the compounds, and nonpolar hydrogen atoms were merged. All torsions of the ligand were allowed to rotate during docking. The value for the exhaustiveness of the search was 400, whereas the number of poses collected was 200. All graphic manipulations and visualizations were performed using the AutoDock Tools 1.5.4 (Sanner, 1999) and ligand docking with Autodock Vina 1.1.1.

#### *Molecular dynamic simulations (MDS)*

The complex geometries from docking were soaked in boxes of explicit water using the TIP3P model (Jorgensen et al., 1983) and subjected to MDS. All MDS were performed with the Amber software package using periodic boundary conditions and cubic simulation cells. The particle mesh Ewald method (Darden et al., 1993) was applied using a grid spacing of 1.2 Å, a spline interpolation order of 4, and a real space direct sum cutoff of 10 Å. The SHAKE algorithm was applied allowing for an integration time step of 2 fs. MDS were carried out at a 300 K target temperature and extended to 20 ns overall simulation time. The isothermal–isobaric (NPT) ensemble was employed using Berendsen coupling to a baro/thermostat (target pressure 1 atm, relaxation time 0.1 ps). Post MD analysis was performed with the program PTRAJ (Case et al., 2005).



### *MM-GBSA free energy decomposition*

To determine the residues of the AChE and BChE catalytic site involved in the interactions, histograms of the interaction energy were used. The MM-GBSA free energy decomposition using the mm\_pbsa program in AMBER12 was employed to corroborate the amino acids interacting with the ligands.

### *QTAIM analysis*

After the QM/MM calculation, the optimized geometries were used as input for QTAIM analysis (Bader, 1985), which was performed with the help of Multiwfn software (Lu and Chen, 2012) using the wave functions generated at the B3LYP-D/6-31G (d) level. This type of calculation has been used in recent studies because it ensures a reasonable compromise between the wave function quality required to obtain reliable values of  $\rho(r)$  and the available computer power, considering the extension of the system in the study (Andujar et al., 2012; Gutierrez et al., 2016; Tosso et al., 2013; Vega-Hissi et al., 2015).

## **Results and discussion**

### *GC-MS analysis of Hieronymiella extracts*

Twenty six compounds suggesting alkaloid structures were detected by comparing their mass fragmentation patterns with standard reference spectra in home-made databases, nineteen of them were identified from their MS data and retention indexes and are listed in Table 1, whereas seven were not recognized among the Amaryllidaceae alkaloids.

Gal was identified in all *Hieronymiella* species in a range of 0.1 – 9.79% (TIC). *H. caletensis* showed the highest relative abundance of Gal followed by *H. marginata* (from Tumbaya) and *H. speciosa* with 4.04 and 3.45%, respectively. Curiously, in *H. clidanthoides* from Tucumán province and *H. marginata* from Volcán district (Jujuy province) species, Gal was not detected. These results are in agreement with previous reports on Amaryllidaceae species showing variability on alkaloid profiles according to the collection site, as *Galanthus elwesii* and *G. nivalis* populations from Bulgaria (Berkov et al., 2011), *Leucojum aestivum* (subsp. *pulchellum*) from Bulgaria and the Balearic Islands (Berkov et al., 2013), as well as *H. jamesoni* from Argentina (Ortiz et al., 2012; Cavallaro et al., 2014). On the other hand, lycorine was detected in all extracts samples, even those from species collected in different locations. It is well known that this compound is the most

occurring Amaryllidaceae alkaloid (Bastida et al., 2011). *H. marginata* from Volcán (Jujuy province) showed the highest abundance of lycorine with 92.98% of TIC. Lycorine possesses a wide range of bioactivities, standing out its ability as inhibitor towards ascorbic acid biosynthesis, organogenesis, growth, and cell division (Bastida et al., 2011).

The bulb extract from *H. aurea* (HE1) showed the highest number of detected alkaloids (sixteen alkaloids, 95.46% of TIC). From them, ten alkaloids were identified by their mass fragmentation pattern and RIs. Gal (**2**) was also detected (2.82% TIC). Haemanthamine/crinamine (**11/12**) and crinan-3-one (**20**) were found in notably high abundance: 42.04% and 19.87% of TIC, respectively. Hemanthamine (**11**) and crinamine (**12**) displayed pronounced cell growth inhibitory activities against a variety of tumor cells, whereas hemanthamine also shown strong antiretroviral activity (Bastida et al., 2006).

Insert Table 1

Regarding *H. caletensis* (HE2), Gal (**2**), tazettinol (**17**), and lycorine (**18**) were identified. It is remarkable the relatively high amount of tazettinol (**17**) and Gal (**2**), with 49.09 and 9.79% of TIC, respectively. This species together with *Zephyranthes filifolia* (Ortiz et al., 2012) represent an important source of Gal (**2**) among Amaryllidaceae from Argentina (supplementary material, Fig. 1S).

Concerning to *H. clidanthoides* (HE3) from Tucumán province, nine alkaloids were detected. Hamayne (**15**)/11-hydroxyvittatine (**16**), lycorine (**18**) and unginorine (**21**) were the most abundant. The alkaloid (**21**) was reported as AChE inhibitor (Ingkaninan y col., 2000). Furthermore, two unknown compounds  $m/z$  289 (**8**) and  $m/z$  344(**10**) were detected. Another sample of this species obtained from La Rioja (HE4) differed notably in its chemical composition (Table 1).

The GC-MS analysis of the three different *H. marginata* samples from Tucumán and Jujuy provinces showed diverse alkaloid profiles, even between those from near places. Among the known alkaloids detected in HE5, sanguinine (**4**) which accounted for 2.63% of TIC, is a galanthamine-type compound with an hydroxyl group at C-9 instead of a methoxyl group that showed an AChE inhibitory activity around 10 times higher than Gal (Lopez et al., 2002). HE5 and HE6 showed a similar alkaloid profile and were characterized by lycorine (**18**) and tazettinol (**17**) as the main alkaloids, together with Gal (**2**), trisphaeridine (**1**) and anhydrolycorine (**7**). Regarding extract HE7, just three alkaloids were identified: chlidanthine (**3**), lycorine (**18**), and anhydrolycorine (**7**), which accounted for 3.18, 92.98, and 0.1% of TIC respectively.

Regarding the *H. speciosa* extract (HE8) the low-occurring alkaloid lycoramine (**5**), was detected in a high abundance (25-30% of TIC). There are discrepancies among different authors regarding its AChE inhibition (Irwin and Smith, 1960; Lopez et al., 2002; Kulhánková et al., 2013).

#### *AChE and BChE inhibitory activity*

The bulb extracts of *H. aurea*, *H. caletensis*, *H. clidanthoides*, *H. marginata*, and *H. speciosa* species were evaluated *in vitro* as inhibitors of AChE and BChE. The results are summarized in Table 2. All the *Hieronimiella* extracts showed strong AChE inhibitory effect ( $IC_{50}$  values  $\leq$  to 15.40  $\mu\text{g/ml}$ ), HE5 being the most potent ( $IC_{50} = 1.84 \mu\text{g/ml}$ ). Furthermore, all these extracts exhibited moderate BChE inhibitory activity ( $IC_{50} = 23.74$ -136.40  $\mu\text{g/ml}$ ), the HE8 and HE5 extracts displaying the highest BChE inhibition ( $IC_{50} = 23.74$  and 36.07  $\mu\text{g/ml}$ , respectively). Since the cholinesterase inhibitory activity of *Hieronimiella* species could be explained by the presence of Gal (**2**), others inhibitor alkaloids as sanguinine (**4**), chlidanthine (**3**), lycoramine (**5**), and unginorine (**21**) can also contribute to the overall extract inhibition, especially in those extracts whose Gal (**2**) content was minor or nonexistent. Thus, the high inhibitory activity of HE5 over AChE could be related to the presence of sanguinine (**4**), the most potent and natural-occurring Amaryllidaceae alkaloid (Lopez et al., 2002). Regarding lycoramine (**5**), a galanthamine-type alkaloid, there is a disagreement among different authors about its AChE inhibitory effect (Irwin and Smith, 1960; Lopez et al., 2002; Kulhánková et al., 2013).

#### Insert Table 2

Considering that both HE6 and HE8 differ notably in the abundance of lycoramine (**5**), (0.85 and 29.84% of TIC, respectively), possess similar abundance of Gal (4.04 and 3.45% of TIC), and have similar  $IC_{50}$  values ( $5.50 \pm 0.01$  and  $5.88 \pm 0.03 \mu\text{g/ml}$ ), these results suggest that lycoramine (**5**) has weak or null inhibitory activity against AChE and support the results of Lopez et al., 2002. On the other hand, these species showed different BChE inhibitory effects, being that of HE8 higher than HE6, suggesting lycoramine (**5**), as a promising BChE inhibitor. Finally, since some alkaloids were not identified in the extracts, they could play a key role on the cholinesterase inhibition of the studied extracts.

The nine isolated alkaloids from *Hieronimyella* species were assayed as inhibitors of AChE and BChE. Although many authors have previously considered that AChE inhibitory effect lesser than 500  $\mu\text{M}$  can be considered as active (Wink, 2000; Elgorashi et al., 2004), herein those alkaloids with  $IC_{50}$  values greater than 200  $\mu\text{M}$  were considered inactive. This trend to the AChE over BChE

inhibition, is in accordance with previous publications (Kulhánková et al., 2013; Cahlíková et al., 2013; Cavallaro et al., 2014) and represent another evidence of the Amaryllidaceae alkaloids selectivity toward AChE. In this regard, Gal (**2**), sanguinine (**4**) and chlidanthine (**3**) showed AChE inhibitory effect ( $IC_{50}$  values = 1.0, 0.1, and 23.50  $\mu$ M, respectively), and weak BChE inhibitory activity ( $IC_{50}$  values = 14, 21.50, and 196.79  $\mu$ M, respectively). The other tested alkaloids did not show inhibitory activity against either enzyme ( $IC_{50} > 200 \mu$ M).

### *Molecular modeling*

To better understand the experimental results, a molecular modeling study on both *Tc*AChE and eqBChE, using combined techniques (Docking calculations, MD simulations, and QTAIM computations) was performed.

Although these studies were conducted with *Tc*AChE instead of *Ee*AChE, several reports have shown that AChE from different species share 65% amino acid sequence homology and similar overall structures (Lee et al., 2007; Khan et al., 2009; Cheung et al., 2012; Brus et al., 2014; Atanasova et al., 2015; Cortes et al., 2015).

Insert Fig. 2

The docking study predicts that all these alkaloids bind in the same region of the active site of AChE; however, MD simulations indicate that these molecules are arranged spatially in several ways and are interacting with different amino acids. Such results might be well appreciated in the analysis *per residue* which has been performed for different compounds (Fig. 2). While the most active compounds sanguinine (Fig. 2a), Gal (Fig. 2b), and chlidanthine interact mainly with Trp84, Gly118, Glu199, Ser200, Phe330, and His440; lycorine (Fig. 2c) produces their main interactions with Tyr70, Asp72, Val71, Trp84, Tyr121, and Ser122. Similar results to those of lycorine were obtained for the rest of inactive isolated alkaloids. It is interesting to note that the alkaloid-amino-acids interactions involved in the active site of AChE are markedly different comparing the galanthamine-type alkaloids to the rest of the simulated alkaloids. These results are in complete agreement with the experimental data and allow us to differentiate between the strong inhibitors from the inactive ones.

However, in order to go further and try to explain the higher inhibitory activity observed for sanguinine respect to Gal and chlidanthine, it is necessary to obtain more accurate and detailed information about the molecular interactions which stabilize and destabilize the ligand-receptor complexes. Thus, QTAIM calculations on the complexes of Gal, sanguinine, and chlidanthine with AChE were performed. The results are presented in Fig. 3 and show the main interactions of these

alkaloids at the binding pocket of AChE. In such figure it is possible to observe that Gal displays six strong stabilizing interactions with the following amino acids: Trp84, Gly118, Glu 199, Ser200, Phe330, and His490 (Fig. 3a). According to the QTAIM analysis,  $\rho(\text{rb})$  values for these interactions are 0.0241, 0.0521, 0.0615, 0.0136, 0.0098, and 0.0065au, respectively. These six interactions are also present in the complex of sanguinine with AChE (Fig. 3b).

Insert Fig. 3

However, for sanguinine the  $\rho(\text{rb})$  values obtained for the same interactions are: 0.025, 0.0352, 0.0685, 0.0345, 0.0088, and 0.017au, respectively. It should be noted that the molecular interactions obtained for sanguinine are stronger than those observed for Gal (supplementary material, Fig. 2S). The exception is the interaction with Gly118 in which the values are higher for Gal. The only structural difference between sanguinine and Gal is the replacement of OCH<sub>3</sub> group by OH. However, such difference allows sanguinine to establish a strong interaction with Ser200. This interaction is missing in Gal due to the exclusive character as proton acceptor of the OCH<sub>3</sub> group. On the basis of our QTAIM study it is reasonable to think that the stronger affinity observed for sanguinine might be attributed to this additional interaction with Ser200 as well as to the stronger molecular interactions observed for sanguinine in comparison to those of Gal for the Glu199 and His440. The differential interactions displayed by the complexes of sanguinine and Gal might be well appreciated in Fig. 3 and supplementary material (Fig. 2S).

It has been reported that the extra hydroxyl group of sanguinine (**4**) available for potential interaction with AChE could explain the strong inhibitory activity of this alkaloid (Lopez et al., 2002). Our results support such hypothesis. The alkaloid chlidanthine (**3**) is a positional isomer of Gal, however it has a very weak inhibitory effect against AChE in comparison to Gal and sanguinine. Our results can explain very well such behavior. While chlidanthine is located practically in the same place of the active site of AChE, their spatial arrangement is very different from those of Gal and sanguinine. This can be clearly seen in Fig. 3c. It is interesting to note that this different spatial ordering is responsible for the weaker interactions of chlidanthine respect to those of sanguinine and Gal (see supplementary material, Fig. 2S). These results are in a complete agreement with the experimental data and allow us to understand the markedly weak inhibitory effect of chlidanthine in comparison to those of sanguinine and Gal.

Likewise, the results obtained for BChE are also in agreement with the experimental data and explain the differential behavior of these alkaloids. Once again the docking study predicts that all these

alkaloids bind in the same region of the active site of BChE and the MD simulations indicate that these molecules are arranged spatially in several ways and are interacting with different amino acids. The Fig. 3Sa shows the analysis *per residue* performed for sanguinine. From this figure it is possible to determine the main stabilizing interactions for the complex sanguinine-BChE; they are with Trp85, Gly118, Glu199, Ser200, Tyr334 and His440. It should be noted that these results are very similar to those recently reported for the interactions of Gal with BChE (Ortiz et al., 2016), indicating that both sanguinine and Gal are good ligands for BChE. In contrast, the results obtained for chlidanthine and lycorine indicate that the stabilizing interactions for the complexes of these alkaloids with BChE are significantly weaker than those observed for sanguinine and Gal (supplementary material, Fig. 3Sb). Similar results were obtained for the rest of inactive alkaloids reported here.

## Conclusions

Argentinean *Hieronymiella* species represent a rich and widespread source of alkaloids, as well as potent AChE and BChE inhibitors. Such activity might be explained at least in part by the content of Gal and sanguinine as well as by other unknown alkaloids. The demand for renewable sources of Gal and other new cholinesterases inhibitors, and the new trend towards the use of natural extracts as medicines instead of pure drugs, could open an avenue for the development of possible Alzheimer disease's treatment by using *Hieronymiella* species.

Furthermore, the results obtained from molecular modeling study, have allowed us to understand at a molecular level the differential behavior of the main alkaloids found in Amaryllidaceae species reported here. Thus, it is possible to explain the higher affinity of Gal and sanguinine over other alkaloids like chlidanthine, lycorine, haemanthamine, and tazettine among others. Besides, the QTAIM studies have also allowed to appreciate more subtle differences in the interactions of each alkaloid among the most active ones; such information can be certainly very useful for the design and search for new inhibitors of cholinesterases, obtained whether from natural sources or by synthesis.

## Conflict of interest

The authors do not have any conflict of interest.

## Supplementary material

Figures S1, S2, and S3

**Acknowledgments**

Research Group 2014-SGR-920 is grateful to the SCT-UB for technical support. J.O. and M.B.A. holds a CONICET grant. G.E.F. and N.B.P. are researchers from CONICET, Argentina. The continuous funding from the UNSL and CONICET is greatly appreciated by RDE and ADG. The authors are grateful to PICTO-UNSJ 2009-116, PICT 2014-3425, and CICITCA-UNSJ, Argentina for the financial support. JB a SCT-UB. The authors acknowledge to Reyes-Chilpa, R.

ACCEPTED MANUSCRIPT

## References

- Anand, P., Singh, B., 2013. A review on cholinesterase inhibitors for Alzheimer's disease. *Arch. Pharm. Res.* 36, 375-399.
- Andujar, S.A., Tosso, R.D., Suvire, F.D., Angelina, E., Peruchena, N., Cabedo, N., Cortes, D., Enriz, R.D., 2012. Searching the “Biologically Relevant” Conformation of Dopamine: A Computational Approach. *J. Chem. Inf. Model.* 52, 99-112.
- Arroyo-Leuenberger, S., Dutilh, J., 2008. Amaryllidaceae. In: Zuloaga, F., Morrone, O., Belgrano, M. (Eds.), *Catálogo de las plantas vasculares del Cono Sur*, pp. 203-226.
- Atanasova, M., Yordanov, N., Dimitrov, I., Berkov, S., Doytchinova, I., 2015. Molecular Docking Study on Galantamine Derivatives as Cholinesterase Inhibitors. *Mol. Inform.* 34, 394-403.
- Bader, R.F.W., 1985. Atoms in molecules. *Acc. Chem. Res.* 18, 9-15.
- Bastida, J., Fernández, J., Viladomat, F., Codina, C., Fuente, G., 1995. Alkaloids from *Narcissus tortuosus*. *Phytochemistry* 38, 549-551.
- Bastida, J., Lavilla, R., Viladomat, F., 2006. Chemical and biological aspects of *Narcissus* alkaloids. In: Cordell, G.A. (Ed.), *The Alkaloids*. Amsterdam, Netherlands, pp. 87-179.
- Bastida, J., Berkov, S., Torras, L., Pigni, N.B., de Andrade, J.P., Martínez, V., Codina, C., Viladomat, F., 2011. Chemical and biological aspects of Amaryllidaceae alkaloids. In: Muñoz-Torrero (Ed.), *Recent Advances in Pharmaceutical Sciences*, Kerala, pp. 65-100.
- Berkov, S., Bastida, J., Sidjimova, B., Viladomat, F., Codina, C., 2011. Alkaloid diversity in *Galanthus elwesii* and *Galanthus nivalis*. *Chem. Biodivers.* 8, 115-130.
- Berkov, S., Georgieva, L., Kondakova V., Viladomat, F., Bastida, Atanassov A., J., Codina, C., 2013. The geographic isolation of *Leucojum aestivum* populations leads to divergation of alkaloid biosynthesis. *Biochem. Syst. Ecol.* 46, 152-161.
- Brus, B., Kosak, U., Turk, S., Pisljar, A., Coquelle, N., Kos, J., Stojan, J., Colletier J.P., Gobec, S., 2014. Discovery, Biological Evaluation, and Crystal Structure of a Novel Nanomolar Selective Butyrylcholinesterase Inhibitor. *J. Med. Chem.* 57, 8167-8179.
- Cahlíková, L., Macáková, K., Kunes, J., Kurfürst, M., Opletal, L., Cvacka, J., Chlebek, J., Blundene, G., 2010. Acetylcholinesterase and butyrylcholinesterase inhibitory compounds from *Eschscholzia californica* (Papaveraceae). *Nat. Prod. Commun.* 5, 1035-1038.



- Case, D.A., Cheatham, T.E., Darden, T., Gohlke, H., Luo, R., Merz, K.M. Jr., Onufriev, A., Simmerling, C., Wang, B., Woods, R.J., 2005. The Amber biomolecular simulation programs. *J. Comput. Chem.* 26, 1668-1688.
- Cavallaro, V., Alza, N.P., Murray, M.G., Murray, A.P., 2014. Alkaloids from *Habranthus tubispathus* and *H. jamesonii*, two Amaryllidaceae with Acetyl- and Butyrylcholinesterase Inhibition Activity. *Nat. Prod. Commun.* 9, 159-162.
- Cheung, J., Rudolph, M.J., Burshteyn, F., Cassidy, M.S., Gary, E.N., Love, J., Franklin, M.C., Height, J.J., 2012. Structures of human acetylcholinesterase in complex with pharmacologically important ligands. *J. Med. Chem.* 55, 10282-10286.
- Cortes, N., Alvarez, R., Osorio, E.H., Alzate, F., Berkov, S., Osorio, E., 2015. Alkaloid metabolite profiles by GC/MS and acetylcholinesterase inhibitory activities with binding-mode predictions of five Amaryllidaceae plants. *J. Pharm. Biomed. Anal.* 102, 222-228.
- Darden, T., York, D., Pedersen, L.J., 1993. Particle mesh Ewald: An Nlog(N) method for Ewald sums in large systems. *Chem. Phys.* 98, 10089-10092.
- Elgorashi, E.E., Stafford, G.I., Van Staden, J., 2004. *Planta Med.* 70, 260-262.
- Ellman, G.L., Courtney, K.D., Andres, V., Featherstone, R.M., 1961. A new and rapid colorimetric determination of acetylcholinesterase activity. *Biochem. Pharmacol.* 7, 88-95.
- Greenblatt, H.M., Kryger, G., Lewis, T.T., Silman, I., Sussman, J.L., 1999. Structure of Acetylcholinesterase Complexed with (-)-Galanthamine at 2.3 Å Resolution. *FEBS Lett.* 463, 321.
- Greig N.H., Lahiri, D.K., Sambamurti, K., 2002. Butyrylcholinesterase: an important new target in Alzheimer's disease therapy. *Int. Psychogeriatr.* 14 Suppl 1, 77-91.
- Gutierrez, L.J., Barrera Guisasola, E.E., Peruchena, N., Enriz, R.D., 2016. A QM/MM study of the molecular recognition site of bapineuzumab toward the amyloid- $\beta$  peptide isoforms. *Mol. Simul.* 42, 196-207.
- Ingkaninan, K., Hazekamp, A., de Best, C.M., Irth, H., Tjaden, U.R., van der Heijden, R., van der Greef, J., Verpoorte, R., 2000. The application of HPLC with on-line coupled UV/MS-biochemical detection for isolation of an acetylcholinesterase inhibitor from narcissus 'Sir Winston Churchill'. *J. Nat. Prod.* 63, 803-806.
- Irwin, R.L., Smith, H.J., 1960. Cholinesterase inhibition by galanthamine and lycoramine. *Biochem. Pharmacol.* 3, 147-148.

- Jorgensen, W.L., Chandrasekhar, J., Madura, J.D., Impey, R.W., Klein, M.L., 1983. Comparison of simple potential functions for simulating liquid water. *J. Chem. Phys.* 79, 926-935.
- Khan, M.T.H., 2009. Molecular interactions of cholinesterases inhibitors using in silico methods: current status and future prospects. *N. Biotechnol.* 25, 331-346.
- Kulhánková, A., Cahlíková, L., Novák, K., Macáková, K., Kuneš, J., Opletal, L., 2013. Alkaloids from *Zephyranthes robusta* Baker and Their Acetylcholinesterase- and Butyrylcholinesterase-Inhibitory Activity. *Chem. Biodivers.* 10, 1120-1127.
- Likhitwitayawuid, K., Angerhofer, C.K., Chai, H., Pezzuto, J.M., Cordell, G.A., Ruangrunsi, N.J., 1993. Cytotoxic and antimalarial alkaloids from the bulbs of *Crinum amabile*. *Nat. Prod.*, 56, 1331-1338.
- Lee, S. S.; Venkatesham, U.; Rao, C. P.; Lam, S. H.; Lin, J. H. 2007. Preparation of secologorins against acetylcholinesterase. *Bioorg. Med. Chem.* 15, 1034–1043.
- López, S., Bastida, J., Viladomat, F., Codina, C., 2002. Acetylcholinesterase inhibitory activity of some Amaryllidaceae alkaloids and *Narcissus* extracts. *Life Sci.* 71, 2521-2529.
- Ortiz, J.E., Berkov, S., Pigni, N.B., Theoduloz, C., Roiman G., Tapia, A., Bastida, J., Feresin, G.E., 2012. Argentinian Amaryllidaceae Wild, a New Renewable Source of Acetylcholinesterase Inhibitor Galanthamine and Other Alkaloids. *Molecules* 17, 13473-13482.
- Ortiz, J.E., Pigni, N.B., Andujar, S., Roitman, G., Suvire, F.D., Enriz, R.D., Tapia, A., Bastida, J., Feresin, G.E., 2016. Alkaloids from *Hippeastrum argentinum* and Their Cholinesterase-Inhibitory Activities: An in Vitro and in Silico Study. *J. Nat. Prod.* 79, 1241-1248.
- Sanner, M.F., 1999. Python: A programming language for software integration and development. *J. Mol. Graph. Model.* 17, 57-61.
- Tosso, R.D., Andujar, S.A., Gutierrez, L., Angelina, E., Rodríguez, R., Nogueras, M., Baldoni, H., Suvire, F.D., Cobo, J., Enriz, R.D., 2013. Molecular Modeling Study of Dihydrofolate Reductase Inhibitors. Molecular Dynamics Simulations, Quantum Mechanical Calculations, and Experimental Corroboration. *J. Chem. Inf. Model.* 53, 2018-2032.
- Trott, O., Olson, A.J., 2010. AutoDock Vina: improving the speed and accuracy of docking with a new scoring function, efficient optimization, and multithreading. *J. Comput. Chem.* 31, 455-461.
- Vega-Hissi, E.G., Tosso, R., Enriz, R.D., Gutierrez, L.J., 2015. Molecular insight into the interaction mechanisms of amino-2H-imidazole derivatives with BACE1 protease: A QM/MM and QTAIM study. *Int. J. Quantum Chem.* 115, 389-397.

- Viladomat, F., Bastida, J., Codina, C., Campbell, W.E., Mathee, S., 1994. Alkaloids from *Brunsvigia josephinae*. *Phytochemistry*, 35, 809-812.
- Wink, M., 2000. Interference of alkaloids with neuroreceptors and ion channels. In: Rahman, A. (Ed.), *Studies in Natural Products Chemistry*, vol. 21. Amsterdam, Elsevier Science, pp. 3-122.
- Zhao, T., Ding, K., Zhang, L., Cheng, X., Wang, C., Wang, Z., 2013. Acetylcholinesterase and Butyrylcholinesterase Inhibitory Activities of  $\beta$ -Carboline and Quinoline Alkaloids Derivatives from the Plants of Genus *Peganum*. *J. Chem.* vol., Article ID 717232, 6 pages, doi:10.1155/2013/717232.

ACCEPTED MANUSCRIPT

**Table 1.** GC-MS data for *Hieronymiella* species alkaloid extracts. Values are expressed as a relative percentage of TIC.

Compound	RI	HE1	HE2	HE3	HE4	HE5	HE6	HE7	HE8	M <sup>+</sup>	MS
trisphaeridine (1)	2275.0	0.1		0.21		0.12	0.11		0.14	223(100)	222(36), 138(26), 224(20), 111(17), 164(17), 137(12), 165(10), 167(10), 166(9)
galanthamine (2)	2413.9	2.82	9.79		0.16	0.10	4.04		3.45	287(83)	286(100), 270(13), 244(24), 230(12), 216(33), 174(27), 115(12)
chlidanthine (3)	2421.6							3.18		287(100)	256(71), 202(62), 286(52), 255(35), 115(35), 165(34), 96(32), 212(31), 160(31)
sanguinine (4)	2428.2					2.63				273(100)	272(86), 160(49), 202(47), 115(22), 256(21), 274(19), 212(17), 152(16), 165(15)
lycoramine (5)	2431.4						0.85		29.84	289 (57)	288(100), 289(58), 115(13), 202(12), 187(11), 44(10), 290(9), 188(9), 189(9), 232(8)
narwedine (6)	2492.4	0.10	1.66				0.65		0.20	285(84)	284(100), 242(18), 216(20), 199(18), 174(31), 128(16), 115(16)
anhydrolycorine (7)	2510.4	0.46	0.10	0.19	0.53	0.10	0.10	0.10	1.39	251(43)	250(100), 192(13), 191(11), 165(4), 164(3), 139(2), 124(7)
<i>m/z</i> 289 (8)	2560.9	0.59		3.36					1.11	289(100)	218(44), 217(35), 260(25), 202 (22), 288(22), 272(21), 201(21), 290(16), 216(16)
deacetylcantabricine (9)	2578.3			4.40						275(100)	204(77), 203(48), 188(36), 187(33), 258(23), 202(23), 246(22), 276(18), 274(18)
<i>m/z</i> 344 (10)	2607.8			14.7						344(100)	345(39), 346(10), 226(58), 75(42), 59(39), 101(37), 161(35), 212(33), 227(31)
haemanthamine/ crinamine <sup>a</sup> (11/12)	2646.6	42.04			2.34					301(14)	272(100), 257(10), 240(16), 181(21), 214(12), 211(14), 128(8)
tazettine (13)	2657.1	0.39			32.27	62.40			25.46	331(23)	298(18), 247(100), 201(18), 181(16), 70(31)
hippamine (14)	2676.6		2.03	2.7	0.20					301(15)	226(100), 227(79), 250(16), 252(13), 300(12), 228(10), 147(9), 268(9), 282(9)
hamayne/ 11-OH-vittatine <sup>a</sup> (15/16)	2712.7	8.22		44.88					0.20	258(100)	181(17), 259(15), 186 (15), 128 (14), 115(13), 211 (13), 242 (10), 214(10), 212(8)
tazettinol (17)	2717.1		49.09			13.64	19.10			317(24)	247(100), 70(33), 71(26), 115(21), 173(20), 201(17), 248(13), 44(13), 230(12)
lycorine (18)	2753.9	3.83	25.77	24.23	57.46	16.32	73.12	92.98	28.21	287(31)	226(100), 227(79), 268(24), 286(19), 250(15), 147(15), 211(7)
<i>m/z</i> 373 (19)	2778.5	1.90								373(100)	374(21), 312(93), 298(63), 212(50), 314(43), 372(41), 375(39), 340(35), 326(32)
crinan-3-one (20)	2843.2	19.87								271(100)	181(54), 270(37), 211(19), 272(17), 153(12), 152(11), 240(10), 238(9), 182(8)
ungiminorine (21)	2883.0			5.19						316(19)	268(100), 212(72), 299(60), 214(57), 242(51), 250(34), 224(24), 225(20), 147(19)
<i>m/z</i> 257 (22)	2899.6	0.67				4.00				257(100)	256(48), 181(26), 258(16), 115(9), 211(8), 153(7), 188(7), 152(7), 128(57)
<i>m/z</i> 271 (23)	2930.9	2.52								271(100)	181(47), 270(33), 211(17), 272(17), 153(10), 152(10), 240(88), 238(87), 182(76)
2-OH-homolycorine (24)	2973.5	8.71								125(100)	96(20), 126(80), 124(55), 94(23), 42(19), 81(16), 82(16), 97(16), 95(15)
<i>m/z</i> 311 (25)	2994.9	0.46								311 (100)	312(186), 310(129), 281(103), 296(76), 280(60), 125(57), 224(55), 268(50),

											238(46)
<i>m/z</i> 297 (26)	3297.9	2.78								297(100)	296(43), 298(16), 149(11), 253(10), 252(10), 282(8), 299(6), 77(6), 251(6)
Total alkaloids	95.46	88.44	99.86	92.96	99.31	97.97	96.26	90.00			

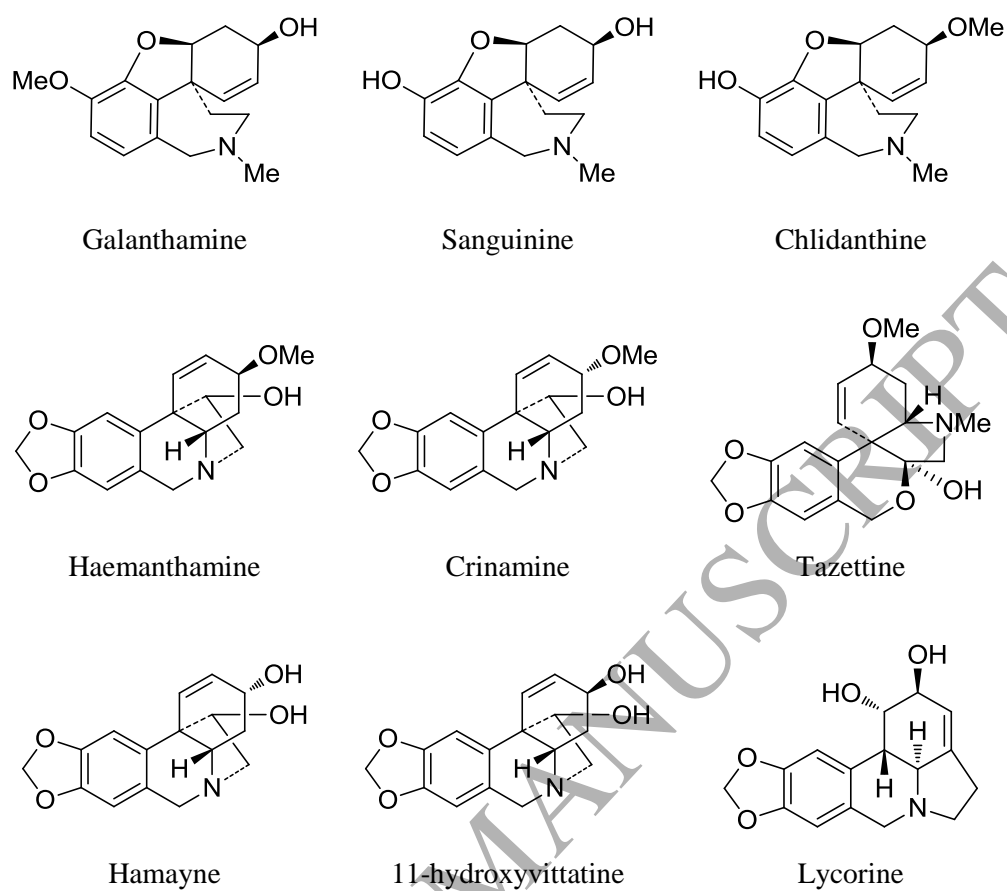
<sup>a</sup>Can not be distinguished by GC-MS. RI: Retention Index. HE1: *Hieronimiella aurea* Extract (Los Cardones, Salta); HE2: *H. caletensis* Extract (Tilcara, Jujuy); HE3: *H. clidanthoides* (Los Quilmes, Tucumán); HE4: *H. clidanthoides* Extract (Chepes, La Rioja); HE5: *H. marginata* Extract (Tafí del Valle, Tucumán); HE6: *H. marginata* Extract (El Volcán, Jujuy); HE7: *H. marginata* Extract (Tumbaya, Jujuy); HE8: *H. speciosa* Extract (San Antonio de los Cobres, Salta).

**Table 2**

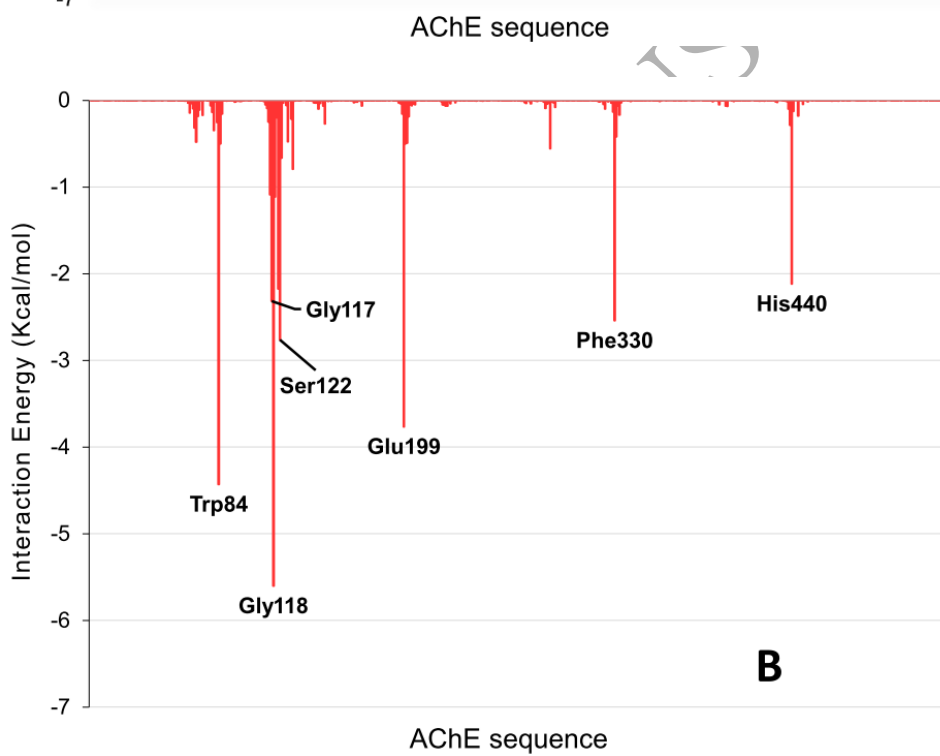
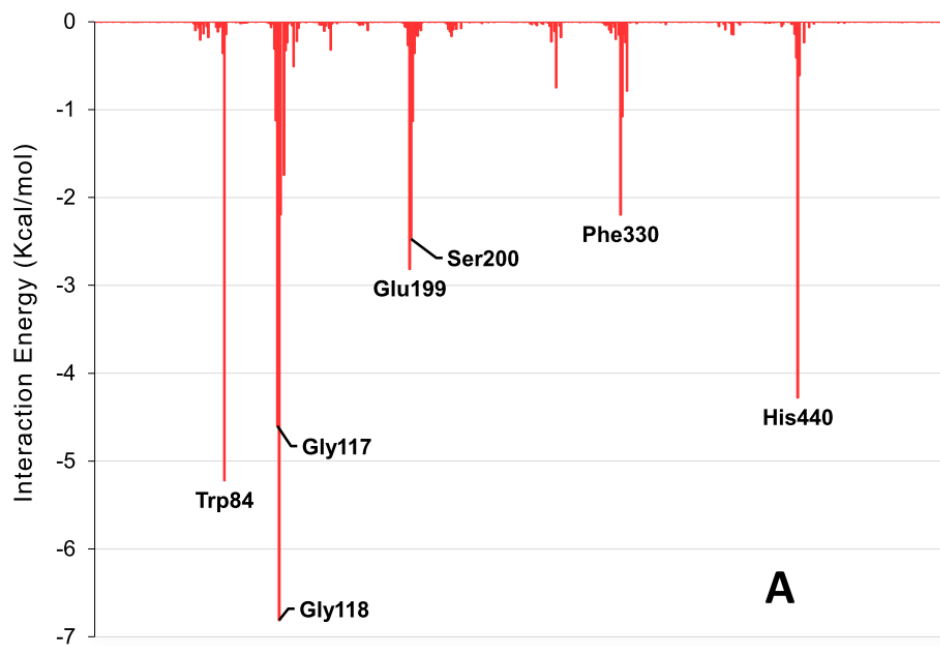
AChE and BChE inhibitory activities of extracts and alkaloids isolated from *Hieronimiella* species, expressed as IC<sub>50</sub> values.

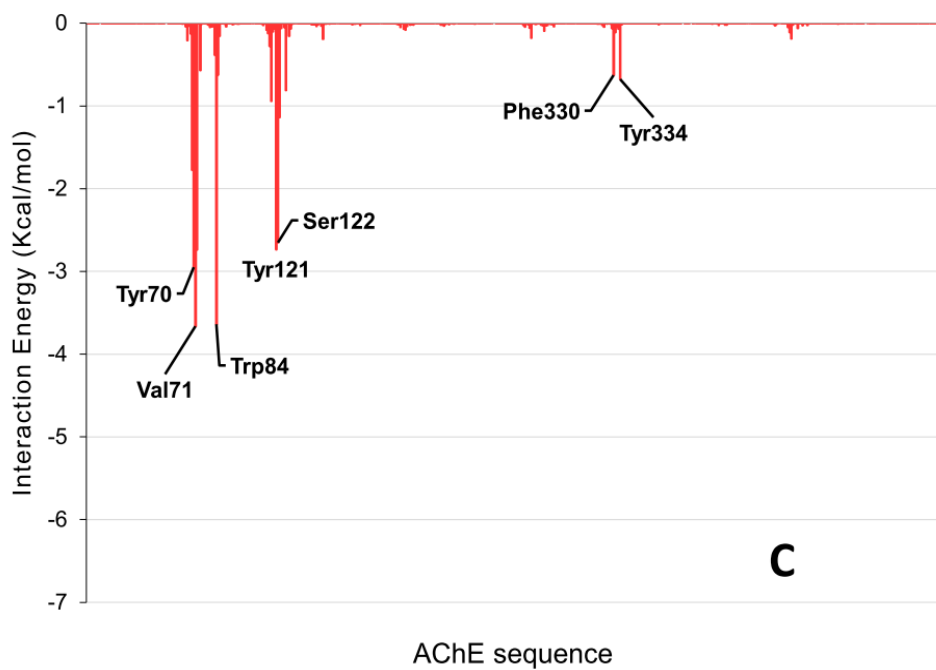
Extracts	IC <sub>50</sub> [μg/ml] <sup>a</sup> of <i>Hieronimiella spp</i> extracts	
	AChE	BChE
HE1	5.84 ± 0.01	>200
HE2	4.80 ± 0.02	106.48 ± 0.05
HE3	15.40 ± 0.02	101.27 ± 0.02
HE4	11.63 ± 0.02	121.86 ± 0.04
HE5	1.84 ± 0.01	36.07 ± 0.02
HE6	5.50 ± 0.01	115.00 ± 0.08
HE7	7.80 ± 0.01	136.40 ± 0.07
HE8	5.88 ± 0.03	23.74 ± 0.02
Isolated Alkaloids	IC <sub>50</sub> [μM] <sup>a</sup>	
haemanthamine (11)	>200	>200
crinamine (12)	>200	> 200
lycorine (18)	>200	>200
11-OH-vittatine (16)	>200	> 200
hamayne (15)	>200	> 200
tazettine (13)	>200	>200
sanguinine (4)	0.10 ± 0.03	21.50 ± 0.04
chlidanthine (3)	23,50 ± 0,65	196,79 ± 2,67
<b>galanthamine (2)<sup>b</sup></b>	<b>1 ± 0.05</b>	<b>14 ± 0.03</b>

<sup>a</sup>IC<sub>50</sub> values are expressed as the means ± SD of three replicate determinations. <sup>b</sup>Reference compound.



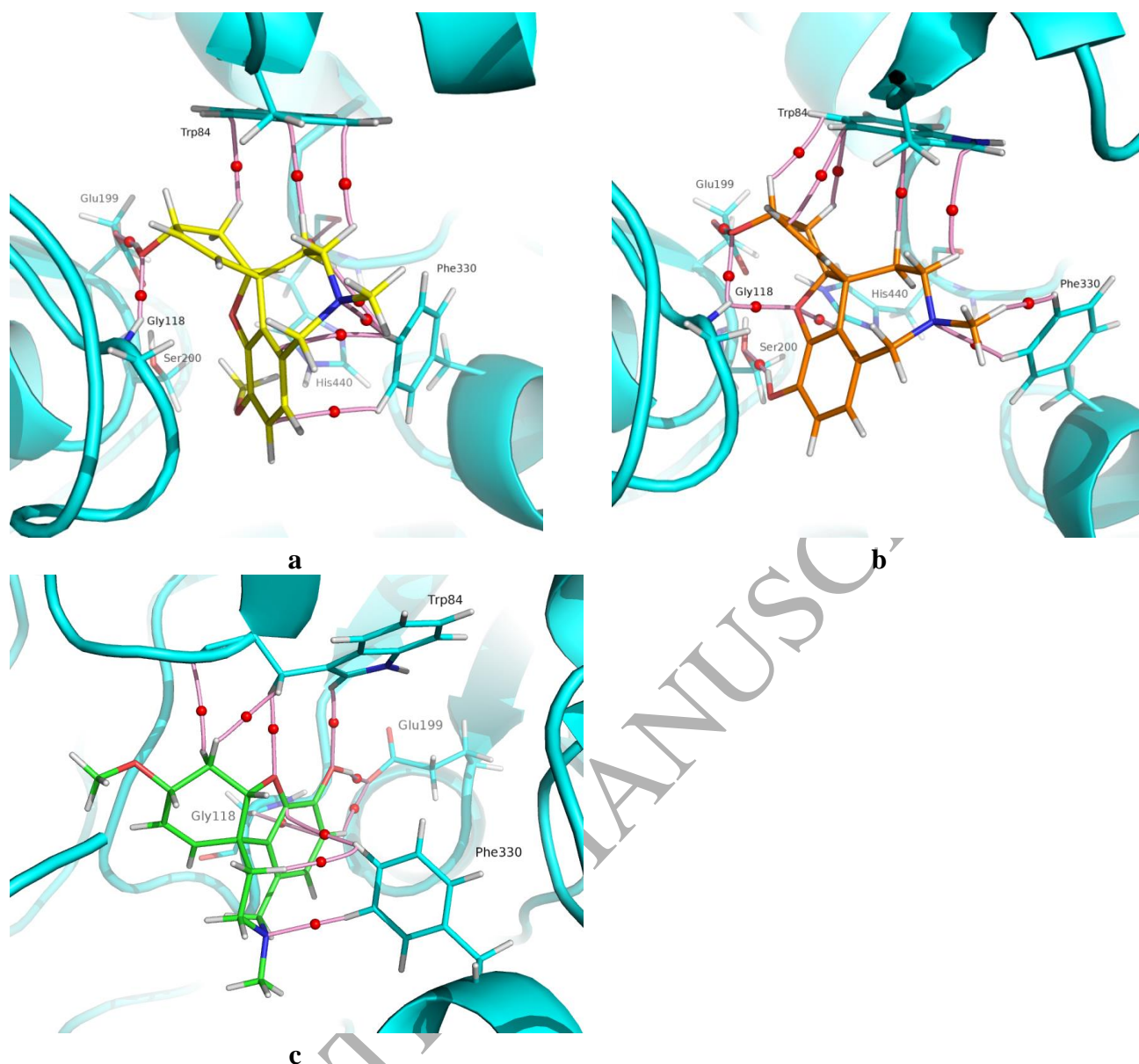
**Figure 1.** Isolated alkaloids from *Hieronymiella* species





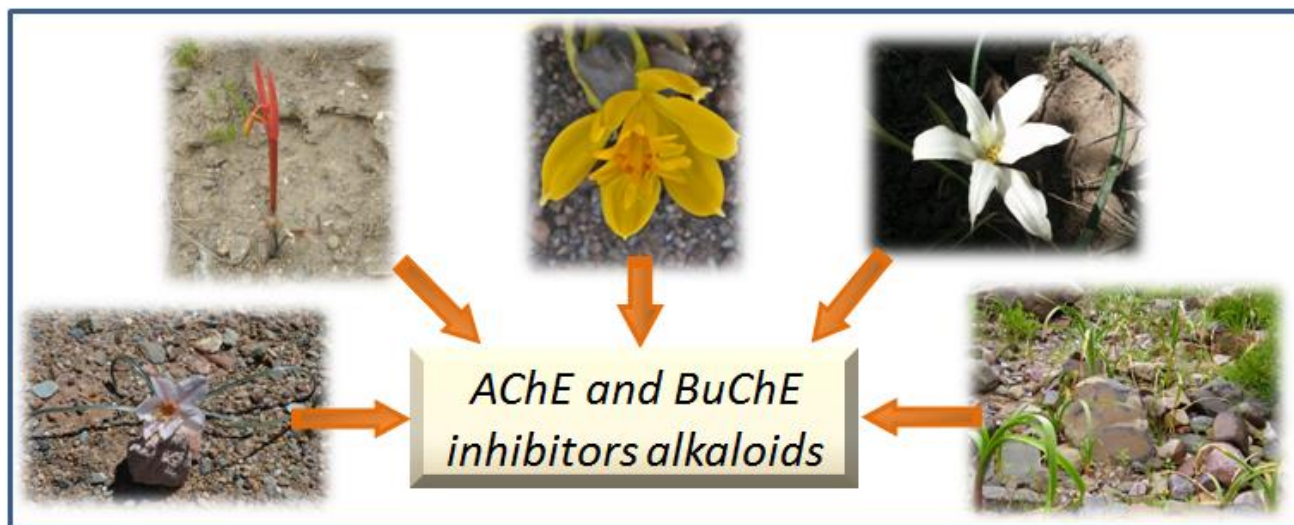
**Figure 2.** Histograms showing the interaction energies of A) Sanguinine, B) Gal, and C) Lycorine with the amino acids involved in the formation of the different complexes with AChE.





**Figure 3.** Molecular graph showing the non-covalent interactions of Gal (a), sanguinine (b), and chlidanthine (c) with the main residues at the binding pocket of AChE. The elements of the topology of the electron density are shown: pink spheres represent the bond paths connecting the nuclei and the critical bond points are represented as red spheres. (For interpretation of the references to colour in this figure legend, the reader is referred to the web version of this article).

## Graphical Abstract



ACCEPTED MANUSCRIPT